

Received 27 October 2015; revised 29 February 2016; accepted 7 March 2016. Date of publication 8 March 2016; date of current version 22 April 2016.  
The review of this paper was arranged by Editor E. Sangiorgi.

Digital Object Identifier 10.1109/JEDS.2016.2539919

# Configurable Electrostatically Doped High Performance Bilayer Graphene Tunnel FET

FAN W. CHEN<sup>1</sup>, HESAMEDDIN ILATIKHAMENEH<sup>2</sup>, GERHARD KLIMECK<sup>2</sup> (Fellow, IEEE),  
ZHIHONG CHEN<sup>3</sup>, AND RAJIB RAHMAN<sup>2</sup>

<sup>1</sup> Network for Computational Nanotechnology, Department of Physics and Astronomy, Purdue University, West Lafayette, IN 47907, USA

<sup>2</sup> Network for Computational Nanotechnology, School of Electrical and Computer Engineering, Purdue University, West Lafayette, IN 47907, USA

<sup>3</sup> Birck Nanotechnology Center, School of Electrical and Computer Engineering, Purdue University, West Lafayette, IN 47907, USA

Fan W. Chen and Hesameddin Ilatikhameneh contributed equally to this work.

CORRESPONDING AUTHORS: F. W. CHEN and H. ILATIKHAMENEH (e-mail: fanchen@purdue.edu; hesam.ilati2@gmail.com)

This work was supported in part by the Center for Low Energy Systems Technology, one of six centers of STARnet, and in part by the Semiconductor Research Corporation Program through Microelectronics Advanced Research Corporation and Defense Advanced Research Projects Agency.

**ABSTRACT** A bilayer graphene-based electrostatically doped tunnel field-effect transistor (BED-TFET) is proposed. Unlike graphene nanoribbon TFETs in which the edge states deteriorate the OFF-state performance, BED-TFETs operate based on bandgaps induced by vertical electric fields in the source, channel, and drain regions without any chemical doping. The performance of the transistor is evaluated by self-consistent quantum transport simulations. This device has several advantages: 1) ultra-low power ( $V_{DD}=0.1V$ ); 2) high performance ( $I_{ON}/I_{OFF}>10^4$ ); 3) steep subthreshold swing ( $SS<10mV/dec$ ); and 4) electrically configurable between N-TFET and P-TFET post fabrication. The operation principle of the BED-TFET and its performance sensitivity to the device design parameters are presented.

**INDEX TERMS** Bilayer graphene (BLG), tunnel field-effect transistor (TFET), electrostatically doping, non-equilibrium Green's function (NEGF).

## I. INTRODUCTION

It has been experimentally challenging to realize a tunnel FET (TFET) with high on-current and a steep subthreshold slope simultaneously, especially with a low supply voltage ( $V_{DD}\sim 0.1V$ ). The high current can be achieved by bringing the transmission probability through the source-channel tunneling barrier close to unity, which can be realized by minimizing the effective mass of the channel material and the screening length [1], [2] across the tunneling barrier. Regarding the requirement of small effective mass, bilayer graphene (BLG) is almost an ideal candidate. However, despite its small effective mass, impressive mobility and initial promise for high performance electronic devices [3], [4], the lack of an intrinsic band gap prevents graphene transistors from switching off. Although sizable bandgaps were demonstrated in graphene nano-ribbons (GNRs) [5]–[8], the edge roughness and device-to-device variations due to the lack of atomic level control in top down fabrication pose a tremendous challenge for technology development [7], [9]–[11]. On the other hand, a tunable bandgap larger than

200meV can be created in BLG by an electric field [12]–[14].

Here, BED-TFET as a high performance steep SS device which enables  $V_{DD}$  to scale down below 0.1V is proposed. Accordingly, an excellent energy-delay product is obtained in this device. Compared to previous bilayer graphene TFET designs [13], [15], BED-TFET has the following advantages: 1) Being electrostatically configurable post fabrication between a P-TFET and a N-TFET. 2) Avoiding the experimentally challenging chemical doping in 2D materials (i.e., bilayer graphene). 3) Being immune to threshold variations due to dopant fluctuations which is critical for low threshold voltages. 4) Avoiding dopant states within the bandgap which deteriorates the OFF-state performance of the TFETs [16]. 5) Providing an artificial heterostructure without interface states.

The device structure is shown in Fig. 1(a). The left and right regions are controlled by  $V_1$ ,  $V_1'$  and  $V_2$ ,  $V_2'$ , respectively, and act as the electrostatically doped source and drain regions for the TFET. By adjusting  $V_1\dots V_2'$ , the proposed

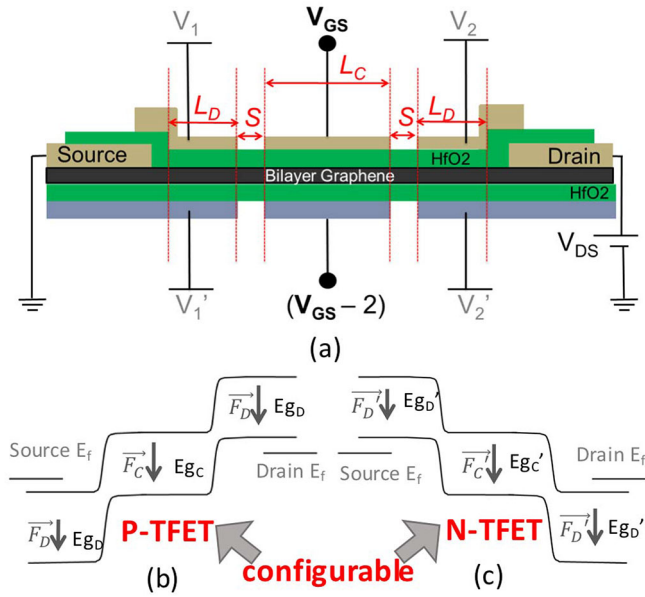


**FIGURE 1.** a) Physical structure of an electrically doped p-i-n BLG TFET. The band diagram in the OFF state of BED-TFET as a b) N-TFET, c) P-TFET.

device is configurable between an N-TFET and a P-TFET as shown in Fig. 1(b) and 1(c). The bandgap size of each region is also tunable by the voltage difference ( $\Delta V$ ) between the top and the bottom gates in that region. The induced band gaps are denoted by  $E_{gC}$  and  $E_{gD}$ . Accordingly, an artificial heterostructure can be made as long as the electric fields of different regions are different,  $\vec{F}_D \neq \vec{F}_C$ . The fabrication of BED-TFET requires the alignment of top and bottom gates, which can be challenging. However, advanced workfunction engineering techniques [17] may be used to reduce the number of gates, however, a detailed investigation of such technique are beyond the scope of this paper.

One of the main advantages of the BED-TFET is its very low energy-delay product. Fig. 2 benchmarks the energy-delay of a 32 bit adder [18] based on different steep devices. The benchmarking methodology is described in [18] for beyond-CMOS devices. The BED-TFET has the least energy-delay product among the studied devices. This is due to the steep IV and high  $I_{ON}$  obtained in the BED-TFET even with a low  $V_{DD}$  of 0.1V. This shows the importance of low band gap materials for low  $V_{DD}$  steep devices. Notice that the parasitic capacitances between the gates can be significantly reduced by using a low-k dielectric ( $\epsilon_S$ ) between the gates [1] and increasing the spacing ( $S$ ); e.g., a 10nm air gap spacer can reduce parasitic capacitances about 2 orders of magnitude smaller than gate capacitance ( $\epsilon_S/S \ll \epsilon_{ox}/t_{ox}$ ). According to Fig. 2, this parasitic capacitance doesn't degrade the energy-delay product of BED-TFET.

## II. SIMULATION DETAILS

The Hamiltonian of BLG is represented using a  $p_z$  orbital nearest-neighbor tight-binding (TB) model, which contains only in-plane and inter-plane hopping terms,  $\gamma_0$  and  $\gamma_1$  as listed in Table 1. The material properties of the BLG under

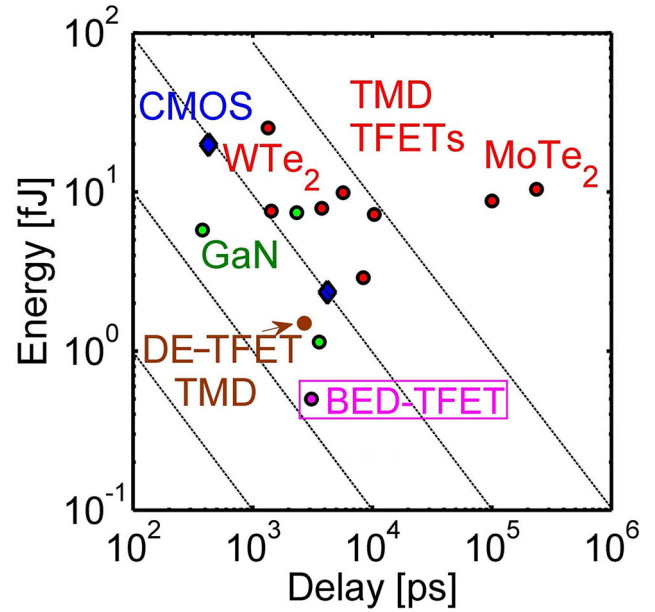


**FIGURE 2.** Energy-Delay comparison of BED-TFET (pink dot) with Dielectric Engineered (DE) WTe<sub>2</sub> TFET (brown dot) [1], Nitride TFET (green dots) [19], TMD TFETs (red dots) [2], [20], [21] and Si MOSFET (blue dots) [18], [22].

vertical field extracted from the bandstructure for the maximum  $E_g$  of 275 meV are also in Table 1. All the transport characteristics of the BED-TFET have been simulated using the self-consistent Poisson-Non Equilibrium Green's Function (NEGF) method through the Nano-Electronic Modeling (NEMO5) tool [23]–[31]. Applying a vertical field to BLG opens up a band gap (Fig. 3).

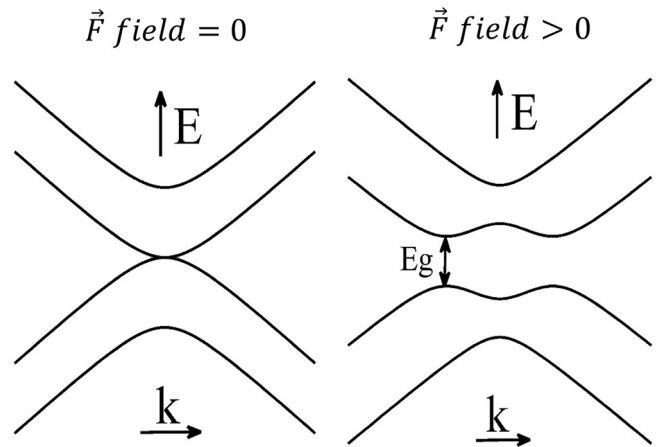


**FIGURE 3.** Vertical electric field opens up a bandgap in BLG.

The BED-TFET shown in Fig. 1a) is composed of a bilayer graphene layer sandwiched between two layers of 3nm thick  $HfO_2$  with a relative dielectric constant of  $\epsilon_r = 20$ . The maximum field within  $HfO_2$  in current BED-TFET design is about 3MV/cm which is less than the breakdown field of  $HfO_2$  ( $\sim 8.5MV/cm$ ) [32]. The three gated regions from left to right have lengths of 25, 40 and 25 nm.  $\Delta V$  in the middle region is fixed to 2V to reach the maximum bandgap (i.e., 275meV in BLG). Notice that,  $V_1 \dots V_2'$  are

fixed throughout the device operation to achieve the desired electrostatically doping. Only the gate voltages in the middle region are swept to switch the device between ON and OFF.

**TABLE 1.** Bilayer graphene material properties: in-plane and inter-plane hopping parameters  $\gamma_0$  and  $\gamma_1$ , maximum bandgap  $E_g$ , electron effective mass  $m_e^*$ , in-plane and out-plane relative dielectric constant  $\epsilon_r^{in}$  and  $\epsilon_r^{out}$ .

Parameters	$\gamma_0$ (eV)	$\gamma_1$ (eV)	$E_g$ (meV)	$\epsilon_r^{in}$	$\epsilon_r^{out}$
Bilayer Graphene	2.75	0.3	275	3	3.3

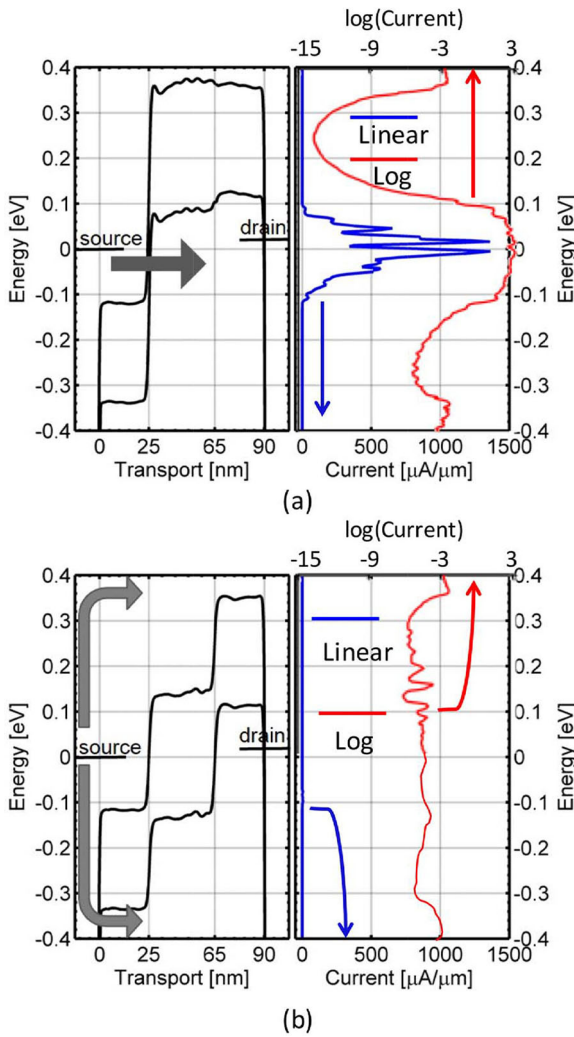


**FIGURE 4.** The band diagram along the transport direction (left) and the energy resolved current (right) in (a) ON state and (b) OFF state.

### III. RESULTS AND DISCUSSION

All the results here are for BED-TFET with P-FET configuration in Fig. 1(b);  $V_1$ ,  $V_1'$  and  $V_2$ ,  $V_2'$  are fixed at 1.1V, -0.1V and 0.4V, -0.8V respectively to form the electrostatically doped source and drain regions.

Fig. 4(a) shows the local band diagram along the transport direction (left) and energy resolved current for the ON-state (right) of the device. There is a tunnel window of about

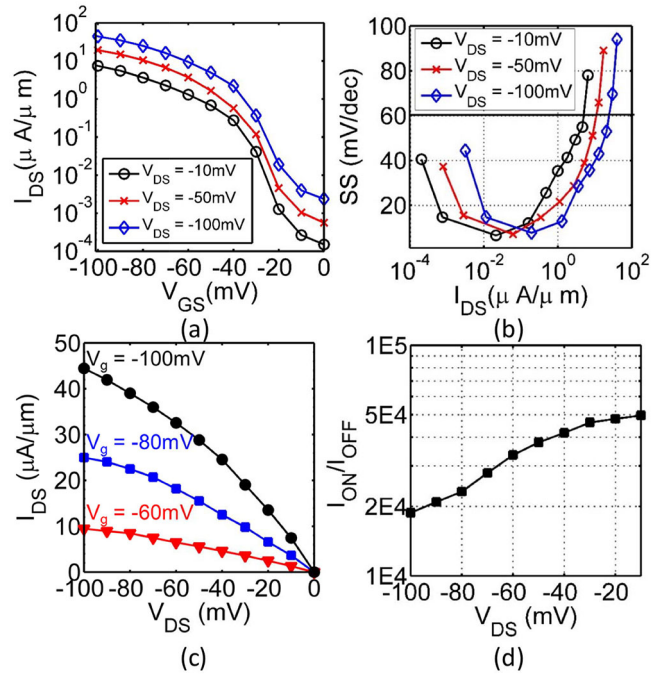


**FIGURE 5.** a) Transfer characteristics of the BED-TFET with different drain-to-source voltages  $V_{DS}$ . b) SS-Id plot with different drain-to-source voltages  $V_{DS}$ . c) Output characteristics of the TFET at several gate voltages  $V_g$ . d) ON/OFF ratio with source-drain voltage  $V_{DS}$  for the BED-TFET.  $L_c$ ,  $L_D$  and  $S$  are kept at 40nm, 25nm and 0nm, respectively.

210 meV in the ON-state. Due to the small band gap at the tunnel junction, the ON-current is high. In the OFF-state, the middle region blocks the tunneling window as shown in Fig. 4(b). Consequently, the OFF-current is mainly the result of the thermionic electron and hole currents. The electrically induced band gaps at the source and drain regions in conjunction with the band gap of the channel make an effective barrier height of about 350meV which is large enough to reduce the thermal current at 300K to the desired range.

Fig. 5(a) shows the transfer characteristics of the BED-TFET for different  $V_{DS}$  values. Increasing  $|V_{DS}|$  from 10mV to 100mV increases both the ON and OFF currents. Fig. 5(b) shows that this device achieves a small SS value of 8 mV/dec and high  $I_{60}$  (the current value where SS becomes 60 mV/dec) value of 24  $\mu\text{A}/\mu\text{m}$  for a  $V_{DS}$  of -100mV. Notice that this value of  $I_{60}$  is much higher than that of other 2D material TFETs even with a  $V_{DD}$  of 0.5V [21]. Notice that increasing  $|V_{DS}|$  from 10mV to 100mV does not deteriorate the small SS. Fig. 5(c) plots the output characteristics of the device.  $I_D$ - $V_{DS}$  curves show that there is no late turn on problem in BED-TFET and the linear region of  $I_D$ - $V_{DS}$  starts from  $V_{DS}=0\text{V}$ . Moreover, the current saturates for  $|V_{DS}|$  values above 50mV. Fig. 5(d) shows that an increase in  $|V_{DS}|$  decreases the ON/OFF ratio from  $5 \times 10^4$  at  $V_{DS}=-10\text{mV}$  to  $2 \times 10^4$  at  $V_{DS}=-100\text{mV}$ , which is not substantial.

Here, tunnel thickness modulation rather than energy filtering is used to achieve steep slope. However, unlike other TFETs that operate with tunnel thickness modulation, the bandgap is dictated locally by the vertical field which is



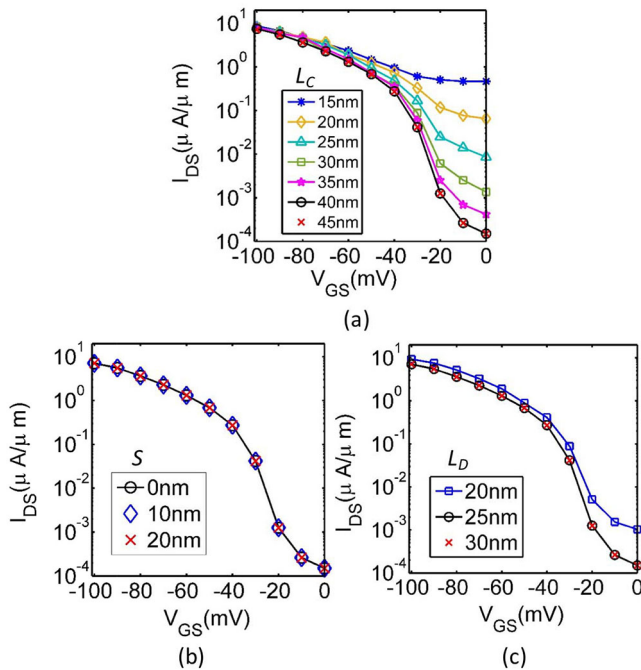


**FIGURE 6.**  $L_D$ ,  $L_C$  and  $L_D$  are the gate length of the left/middle/right region in Fig. 1(a) (doping region/channel/doping region), respectively. The spacing between the gates is  $S$ . Transfer characteristics of the TFET with different a) channel length  $L_C$  ( $L_D = 25\text{nm}$ ,  $S = 0\text{nm}$ ), b) spacing  $S$  ( $L_C = 40\text{nm}$ ,  $L_D = 25\text{nm}$ ) and c) doping region length  $L_D$  ( $L_C = 40\text{nm}$ ,  $S = 0\text{nm}$ ).

smaller at the source-channel interface than in the channel. Consequently, a larger current can be achieved in this TFET. Notice that the energy filtering mechanism is not effective in low bandgap materials since the small gap can only block a small portion of the Fermi tail.

In the BED-TFET, several design parameters are identified to be critical for the device performance and fabrication: 1) the channel length  $L_C$ , 2) the length of the electrostatically doped source and drain regions  $L_D$ , and 3) the spacing between these gated regions  $S$ . In the transfer characteristics demonstrated in Figs. 6a-c,  $L_C$ ,  $L_D$  and  $S$  are kept at 40nm, 25nm and 0nm respectively, unless mentioned otherwise. Fig. 6(a) shows that reducing  $L_C$  to 40nm increases the OFF-current. Below, the performance is not sensitive to  $S$  as shown in Fig. 6(b) for  $S$  in the range of 0nm to 20nm. Fig. 6(c) shows that a  $L_D$  value below 25nm can impact the OFF-state performance. The sensitivity to  $L_C$  and  $L_D$  originates from the direct tunneling of carriers through the channel potential barrier due to the small effective mass of the BLG. The optimized channel length is longer than the ITRS requirements. Hence, to keep the footprint of the BED-TFET small a vertical structure (e.g., conventional vertical TFET structure [33]) could be used.

#### IV. CONCLUSION

In this work, the BED-TFET is proposed as a high performance, ultra-low power, steep transistor to overcome the problems associated with GNRs. The electrically tunable

band gap of BLG makes this transistor highly configurable. The performance of this device is evaluated through rigorous quantum transport simulations based on NEGF. It is shown that with the right device design, the BED-TFET can achieve ON/OFF ratios of more than  $10^4$ , ON-current of  $45\mu\text{A}/\mu\text{m}$ , and a subthreshold swing around 10 mV/dec, all at a low overdrive voltage of  $V_{DD} = 0.1\text{V}$  at room temperature.

#### ACKNOWLEDGMENT

The authors would like to thank J. Nahas and R. Perricone for the 32-bit adder energy-delay calculations.

#### REFERENCES

- [1] H. Ilatikhameh, T. A. Ameen, G. Klimeck, J. Appenzeller, and R. Rahman, "Dielectric engineered tunnel field-effect transistor," *IEEE Electron Device Lett.*, vol. 36, no. 10, pp. 1097–1100, Oct. 2015.
- [2] H. Ilatikhameh, G. Klimeck, J. Appenzeller, and R. Rahman, "Scaling theory of electrically doped 2D transistors," *IEEE Electron Device Lett.*, vol. 36, no. 7, pp. 726–728, Jul. 2015.
- [3] T. Ohta, A. Bostwick, T. Seyller, K. Horn, and E. Rotenberg, "Controlling the electronic structure of bilayer graphene," *Science*, vol. 313, no. 5789, pp. 951–954, Aug. 2006.
- [4] F. Schwierz, "Graphene transistors," *Nat. Nanotechnol.*, vol. 5, no. 7, pp. 487–496, 2010.
- [5] Z. Chen, Y.-M. Lin, M. J. Rooks, and P. Avouris, "Graphene nanoribbon electronics," *Phys. E Low Dimensional Syst. Nanostruct.*, vol. 40, no. 2, pp. 228–232, Dec. 2007.
- [6] M. Y. Han, B. Özyilmaz, Y. Zhang, and P. Kim, "Energy band-gap engineering of graphene nanoribbons," *Phys. Rev. Lett.*, vol. 98, no. 20, May 2007, Art. no. 206805.
- [7] M. Luisier and G. Klimeck, "Performance analysis of statistical samples of graphene nanoribbon tunneling transistors with line edge roughness," *Appl. Phys. Lett.*, vol. 94, no. 22, Jun. 2009, Art. no. 223505.
- [8] F. Liu, X. Liu, J. Kang, and Y. Wang, "Improved performance of tunneling FET based on hetero graphene nanoribbons," *arXiv preprint arXiv:1312.3391*, 2013.
- [9] D. Basu, M. J. Gilbert, L. F. Register, S. K. Banerjee, and A. H. MacDonald, "Effect of edge roughness on electronic transport in graphene nanoribbon channel metal-oxide-semiconductor field-effect transistors," *Appl. Phys. Lett.*, vol. 92, no. 4, Jan. 2008, Art. no. 042114.
- [10] G. Fiori and G. Iannaccone, "Simulation of graphene nanoribbon field-effect transistors," *IEEE Electron Device Lett.*, vol. 28, no. 8, pp. 760–762, Aug. 2007.
- [11] Y. Yoon and J. Guo, "Effect of edge roughness in graphene nanoribbon transistors," *Appl. Phys. Lett.*, vol. 91, no. 7, Aug. 2007, Art. no. 073103.
- [12] T. Chu and Z. Chen, "Achieving large transport bandgaps in bilayer graphene," *Nano Res.*, vol. 8, no. 10, pp. 3228–3236, 2015.
- [13] G. Fiori and G. Iannaccone, "Ultralow-voltage bilayer graphene tunnel FET," *IEEE Electron Device Lett.*, vol. 30, no. 10, pp. 1096–1098, Oct. 2009.
- [14] J. Nilsson, A. H. C. Neto, F. Guinea, and N. M. P. Peres, "Electronic properties of graphene multilayers," *Phys. Rev. Lett.*, vol. 97, no. 26, 2006, Art. no. 266801.
- [15] T. K. Agarwal *et al.*, "Bilayer graphene tunneling FET for sub-0.2 V digital CMOS logic applications," *IEEE Electron Device Lett.*, vol. 35, no. 12, pp. 1308–1310, Dec. 2014.
- [16] S. Agarwal and E. Yablonovitch, "Band-edge steepness obtained from Esaki/backward diode current-voltage characteristics," *IEEE Trans. Electron Devices*, vol. 61, no. 5, pp. 1488–1493, May 2014.
- [17] O. Weber *et al.*, "Work-function engineering in gate first technology for multi-VT dual-gate FDSOI CMOS on UTBOX," in *Proc. IEEE Int. Electron Devices Meeting (IEDM)*, San Francisco, CA, USA, 2010, pp. 3.4.1–3.4.4.
- [18] D. E. Nikonov and I. A. Young, "Benchmarking of beyond-CMOS exploratory devices for logic integrated circuits," *IEEE J. Explor. Solid-State Computat. Devices Circuits*, vol. 1, no. 1, pp. 3–11, Dec. 2015.

- [19] W. Li *et al.*, "Polarization-engineered III-nitride heterojunction tunnel field-effect transistors," *IEEE J. Explor. Solid-State Computat. Devices Circuits*, vol. 1, no. 1, pp. 28–34, Dec. 2015.
- [20] H. Ilatikhameneh, R. Rahman, J. Appenzeller, and G. Klimeck, "Electrically doped WTe<sub>2</sub> tunnel transistors," in *Proc. SISPAD*, Washington, DC, USA, 2015, pp. 270–272.
- [21] H. Ilatikhameneh *et al.*, "Tunnel field-effect transistors in 2-D transition metal dichalcogenide materials," *IEEE J. Explor. Solid-State Computat. Devices Circuits*, vol. 1, no. 1, pp. 12–18, Dec. 2015.
- [22] M. Salmani-Jelodar, S. R. Mehrotra, H. Ilatikhameneh, and G. Klimeck, "Design guidelines for sub-12 nm nanowire MOSFETs," *IEEE Trans. Nanotechnol.*, vol. 14, no. 2, pp. 210–213, Mar. 2015.
- [23] F. W. Chen *et al.*, "Transport properties of bilayer graphene field effect transistor," in *Proc. TECHCON*, Austin, TX, USA, 2015.
- [24] F. W. Chen *et al.*, "Achieving a higher performance in bilayer graphene FET—Strain engineering," in *Proc. Int. Conf. Simulat. Semicond. Process. Devices (SISPAD)*, Washington, DC, USA, 2015, pp. 177–181.
- [25] F. W. Chen *et al.*, "In-surface confinement of topological insulator nanowire surface states," *Appl. Phys. Lett.*, vol. 107, no. 12, Sep. 2015, Art. no. 121605.
- [26] J. E. Fonseca *et al.*, "Efficient and realistic device modeling from atomic detail to the nanoscale," *J. Comput. Electron.*, vol. 12, no. 4, pp. 592–600, Dec. 2013.
- [27] K. Miao *et al.*, "Büttiker probes for dissipative phonon quantum transport in semiconductor nanostructures," *arXiv preprint arXiv:1508.06657*, 2015.
- [28] H. Ilatikhameneh, F. W. Chen, R. Rahman, and G. Klimeck, "Electrically doped 2D material tunnel transistor," in *Proc. IWCE*, West Lafayette, IN, USA, 2015, pp. 1–3.
- [29] F. W. Chen, M. J. Manfra, G. Klimeck, and T. C. Kubis, "NEMO5: Why must we treat topological insulator nanowires atomically?" in *Proc. IWCE*, West Lafayette, IN, USA, 2015.
- [30] T. Chu, H. Ilatikhameneh, G. Klimeck, R. Rahman, and Z. Chen, "Electrically tunable bandgaps in bilayer MoS<sub>2</sub>," *Nano Lett.*, vol. 15, no. 12, pp. 8000–8007, 2015.
- [31] H. Ilatikhameneh, G. Klimeck, and R. Rahman, "Can homojunction tunnel FETs scale below 10 nm?" *IEEE Electron Device Lett.*, vol. 37, no. 1, pp. 115–118, Jan. 2016.
- [32] L. Kang *et al.*, "Electrical characteristics of highly reliable ultrathin hafnium oxide gate dielectric," *IEEE Electron Device Lett.*, vol. 21, no. 4, pp. 181–183, Apr. 2000.
- [33] R. Gandhi, Z. Chen, N. Singh, K. Banerjee, and S. Lee, "Vertical si-nanowire n-type tunneling FETs with low subthreshold swing (< 50mV/decade) at room temperature," *IEEE Electron Device Lett.*, vol. 32, no. 4, pp. 437–439, Apr. 2011.



**FAN W. CHEN** received the bachelor's degree in physics from Fudan University, Shanghai, in 2011. She is currently pursuing the Ph.D. degree with Purdue University, West Lafayette, IN, USA. She had past experience on condensed matter experiments. Since 2012, she has been specializing in quantum transport simulation, involved with new materials such as topological insulator (Bi<sub>2</sub>Te<sub>3</sub>), bilayer graphene, TMDs, and phosphorene. Her focus is to understand the material properties, device physics and achieve steep slope device with

novel tunnel FET designs. She is currently a leading Researcher in modelling the transport of vertically stacked 2-D materials in LEAST center.

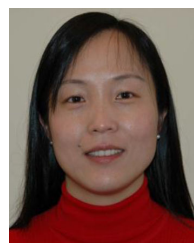


**HESAMEDDIN ILATIKHAMENEH** received the M.S. degree in electrical engineering from Sharif University, Tehran, Iran, in 2007. He is currently pursuing the Ph.D. degree with Purdue University, West Lafayette, IN, USA. He conducts research on the novel electronic, thermoelectric, and optoelectronic devices to predict the performance and understand the underlying physics of these devices. He has also been an Active Member of LEAST Project with the purpose of realizing steep subthreshold devices. He is currently a member of NEMO5 Development Team and has been involved in the development of quantum transport, strain, mode-space, and phonon solvers for this tool.

His current research interests include ultrascaled Si, III-V, and 2-D materials FETs and tunnel FETs, nitride hetero-structures, quantum dots, quantum transport, and scaling theories.



**GERHARD KLIMECK** (S'91–M'95–SM'04–F'13) received the Ph.D. degree from Purdue University, in 1994, and the German electrical engineering degree from Ruhr-University Bochum, in 1990. He is the Reilly Director of the Center for Predictive Materials and Devices and Network for Computational Nanotechnology and a Professor of Electrical and Computer Engineering with Purdue University. He was the Technical Group Supervisor for the Applied Cluster Computing Technologies Group, NASA Jet Propulsion Laboratory. He was a Technical Staff Member with the Central Research Laboratory, Texas Instruments. He has been the lead on the development of NEMO 3-D, a tool that enables the simulation of tens-of-million atom quantum dot systems, and NEMO 1-D, the first nanoelectronic CAD tool. He leads the development and deployment of web-based simulation tools, research seminars, tutorials, and classes that are hosted on <http://nanohub.org> a National Nanotechnology Resource and Infrastructure Community website that is utilized by over 330 000 users annually. He has co-authored 35 tools on nanoHUB that have been used by over 41 000 users. Over 11 000 students used these tools in formalized educational settings such as homework or project assignments in over 776 courses at 64 institutions. His lectures and tutorials have been viewed by over 274 000 nanoHUB users. His work is documented in over 440 peer-reviewed publications and over 670 conference presentations. His research interest is in the modeling of nanoelectronic devices, parallel computing, and the study of user behavior and assessment. He is also a fellow of the Institute of Physics and the American Physical Society.



**ZHIHONG CHEN** is an Associate Professor of Electrical and Computer Engineering with Purdue University, since 2010. Her research focuses on understanding physical properties of nanomaterials, fabricating nano-structures with desired properties and functionalities for electronic, spintronic, and optoelectronic applications. From 2004 to 2010, she was with the IBM T. J. Watson Research Center working on design and fabrication of high performance carbon-based electronics. She was appointed as the Manager of the Carbon

Technology Group from 2008 to 2010. She is an Associate Editor of the IEEE ELECTRON DEVICE LETTERS.



**RAJIB RAHMAN** received the bachelor's degree in physics from Gettysburg College, in 2002, and the master's and Ph.D. degrees in electrical engineering from Purdue University, in 2005 and 2009, respectively. From 2009 to 2012, he was a Post-Doctoral Fellow with Sandia National Laboratories, where he investigated quantum computing architectures in silicon. He is currently a Research Assistant Professor with Purdue University, working on atomistic modeling of electronic structure and transport properties of nanoscale devices. He is one of the developers of the NEMO3D tool. His current research focuses on spin relaxation and many-body interactions in semiconductor qubits, and device applications of 2-D materials.